

MULTI-ELECTRODE TRANSCUTANEOUS ELECTRICAL STIMULATION OF THE HUMAN EXTERNAL EAR

SKOZIKOŽNA STIMULACIJA ZUNANJEGA ČLOVEŠKEGA UŠESA Z VEČ ELEKTRODAMI

**Polona Pečlin¹, Janez Rozman^{2,3*}, Renata Janež³, Anja Emri⁴, Samo Ribarič³,
Tomislav Mirković⁵**

¹University Medical Centre Ljubljana, Division of Gynaecology and Obstetrics, Šljajmerjeva 3 and Zaloška 7, 1000 Ljubljana, Slovenia

²Center for Implantable Technology and Sensors, ITIS d. o. o. Ljubljana, Lepi pot 11, 1000 Ljubljana, Slovenia

³University of Ljubljana, Institute of Pathophysiology, Faculty of Medicine, Zaloška 4, 1000 Ljubljana, Slovenia

⁴Medical Chamber of Slovenia, Dunajska cesta 162, 1000 Ljubljana, Slovenia

⁵University Medical Centre Ljubljana, Department of Anaesthesiology and Surgical Intensive Therapy, Zaloška 2, 1000 Ljubljana, Slovenia

Prejem rokopisa – received: 2023-01-31; sprejem za objavo – accepted for publication: 2023-02-21

doi:10.17222/mit.2023.779

This article reviews the development of a new concept for crafting and testing a multi-electrode set-up for selective transcutaneous auricular nerve stimulation (tANS) using particular superficial regions of the external ear (EE). The purpose of the work is to assess the mechanical properties of the set-up to ensure the optimum conditions for the users, and to test the ability to affect vital physiological functions. The set-up consisted of eight cap-like platinum simulating cathodes ($S = 14.58 \text{ mm}^2$) that were embedded in the left and right silicone ear plugs. The plugs were mounted onto the frame of dummy headphones and inserted into the EE, while a common anode (anode) ($S = 4500 \text{ mm}^2$) was placed at the nape of the neck. The mechanical performance was assessed by measuring the axial force F_x acting on each cathode against the bending of the dummy headphone frame while simulating the conditions of the set-up being mounted onto the head. The functionality was tested by applying stimuli onto four predefined sites at the EE to modify particular vital physiological functions of female volunteers. The preliminary results show that during the tANS, the bi-nasal respiration became shorter but more frequent with steeper inspiration and a lower airflow. The results also show that during the tANS, the heart rate was slightly diminished along with the respiratory sinus arrhythmia. Finally, a dicrotic notch within the toe photoplethysmogram was masked by the waves with a frequency of approximately 300 min^{-1} . The presented work has implications for the multi-electrode set-up design and the prediction of efficient tANS used to modify physiological functions.

Keywords: platinum stimulating electrode, spot welding, transcutaneous auricular nerve stimulation, physiological function

Članek opisuje razvoj novega koncepta izdelave in testiranja večelektrodnega sistema za skozikožno stimulacijo avrikularnega živca (tANS) preko posameznih površinskih področij zunanega ušesa (EE). Namen raziskave je bil izmeriti mehanske lastnosti sistema, da bi zagotovili optimalne pogoje za uporabnike ter testirati zmožnosti sistema vplivanja na fiziološke življenjske funkcije. Sistem je vseboval osem platinastih stimulacijskih katod v obliki kapice ($S = 14,58 \text{ mm}^2$), ki so bile vgrajene v levi in desni ušeni vstavek iz silikona. Vstavka sta bila vgrajena na okvir slušalk in vstavljena v EE, skupna anoda (anode) ($S = 4500 \text{ mm}^2$) pa je bila nalepljena na tilnik. Mehanske lastnosti so bile pridobljene z merjenjem aksialne sile F_x , ki je ob ukrivljanju okvirja slušalk delovala na vsako od stimulacijskih katod pri čemer so bile mehanske razmere, ko je bil sistem nataknen na glavo, simulirane. Funkcionalnost je bila preizkušena z dovajanjem stimulusov na štiri prednastavljena mesta na EE prostovoljk pri čemer so s stimulacijo teh mest vplivali na fiziološke funkcije. Predhodni rezultati so pokazali, da je bilo predihavanje skozi obe nosnici med tANS krajše in pogostejše ter bolj strmo s plitvejšimi vdih. Rezultati so tudi pokazali, da sta bila med tANS rahlo zmanjšana tako ritem srca kakor tudi predihovalna sinusna aritmija. Dikrotični prevoj v pletizmogramu izmerjenem na palcu leve noge je bil prekrit z valovi frekvence približno 300 min^{-1} . Predstavljeno delo ima posledično vpliv na razvoj večelektrodnih sistemov in na pričakovano učinkovitost vplivanja na fiziološke funkcije.

Ključne besede: platinasta stimulacijska elektroda, točkovno varjenje, skozikožna stimulacija avrikularnega živca, fiziološka funkcija

1 INTRODUCTION

Vagus nerve stimulation (VNS) is a stimulation method that is used to treat various diseases.¹ VNS refers to any technique used to stimulate the parasympathetic vagus nerve.²⁻⁴

Invasive VNS, which was approved in the early 1990s, was established as a safe and effective technique, particularly for epilepsy. However, because invasive VNS requires anaesthesia, it may cause surgical risks

during device implantation. With regard to this factor, a myriad of models and methods for a non-invasive interface between the human nervous system and electronic devices have been developed. An example of this method is transcutaneous vagus nerve stimulation (tVNS) which can elicit similar therapeutic effects. The tVNS is used in the application of electrical currents via surface electrodes at selected locations such as tragus, concha and cymba concha with cutaneous afferent vagus nerve distributions.⁵ However, the optimal location and the stimulation parameters that provide the desired therapeutic effects for a specific condition are still speculative.^{6,7}

*Corresponding author's e-mail:
jnzzmn6@gmail.com (Janez Rozman)

The tVNS method has been recently suggested as an interesting alternative for generating effects for a specific condition.^{1,6,7} Recent studies have revealed that the tANS can modulate vagal afferents within the auricular branch of the vagus nerve that may be accessed through particular sites of the external ear (EE).⁸

However, the existing set-up designs do not have the ability to selectively modulate the function of a particular internal organ via the tANS of particular populations of nerve fibres, located in the EE. A disadvantage of such multi-electrode tANS set-ups may be related to the design, composition of the electrode material, and surface properties while being in contact with the human skin.⁹ All the tANS applications require electrodes that ensure an appropriate electrode-tissue interface and appropriate interactions with the skin to avoid any unpleasant feelings or pain. This interface mainly depends on the quality of the physical contact made by a particular stimulating electrode, established by the pressure applied during the tANS. Since the stimulation intensity provides some control of the variation in the electrode-tissue impedance, the intensity of the tANS is usually set according to the patient-specific pain threshold. As it is necessary that the materials used for tANS electrodes enable the functioning in electrochemically harsh environments, an understanding of the electrode-tissue interface and its interactions is necessary.¹⁰ Therefore, the material used and the modification techniques that may be used to optimize the surface and properties of the materials should be identified.^{10–14}

The basic motivation for the work was the desire to generate therapeutic effects on chronic disease patients in a selective way and with the aim of re-establishing the diminished function of particular internal organs using the single-part multi-electrode tANS set-up.⁶ Precisely, the motivation for the proposed work was the necessity to overcome the disadvantage of the existing tANS set-ups that were designed to have up to three electrodes in different configurations to enable tANS of an EE at one or two particular sites. We also intended to increase the understanding of the electrode-tissue interface.

The significance of our work is related specifically to the desire to affect the respiratory and cardiovascular function using the selective tANS of afferent nerve fibres located at particular sites on the EE. This indicates the potential for therapeutic effects on cardiovascular disease patients.

Most research groups generally report on the use of tANS set-ups designed in such a way that they have, at the most, one monopolar or two bipolar electrodes to stimulate one or two particular sites on the EE.^{7,8} In most cases, their technical specifications are not provided.⁹

Some studies do not provide sufficient information about the tANS electrodes such as the material and size

of the electrodes, especially when they are integrated in custom-made set-ups.^{7–9} As a result, an adequate description of the electrode-tissue interface and its interactions is not provided.

Among the metallic materials for stimulating electrodes, titanium and silver are the most commonly used materials.^{6,12,13}

As the reported tANS set-ups generally include only a few stimulating electrodes to stimulate the EE, single-part systems with a larger number of electrodes are required.

To address these needs, an entire conceptual model for crafting a multi-electrode set-up for the selective tANS of afferent nerve fibres within particular sites of the EE was developed based on the theoretical background.

Pure platinum (99.93 w/%) with superior electro-chemical properties may be used as the material to make stimulating electrodes.¹⁰ Except for the low strength, pure platinum exhibits several physical properties of great significance, allowing its use in the tANS electrode crafting. A cold-rolled thin platinum ribbon that underwent different thermal treatments may be proposed for the crafting process^{11–14} to overcome the inadequate properties. For the crafting process, plastic deformation of a thin platinum ribbon with a custom-designed tool and pressing device may be envisaged.

The resistance spot welding and custom-designed tool were proposed to connect the electrodes to the lead wires.^{15–17} For this purpose, a custom-designed capacitive-discharge welding device would be used. This approach would significantly reduce the time required for welding, and thus, the melting spots would be small, and only a small number of heat-affected zones would exist.

For the set-up, reusable earplugs made of soft and sterilisable silicone should be installed onto a frame unmounted from audio headphones. Plugs used by swimmers should be used as the basis for mounting the stimulating electrodes onto predefined sites.

According to the motivation for the work, three aims were set as mentioned below.

The first aim is to develop a set-up that exhibits appropriate mechanical features, ensuring that the system can generate an optimum pressure onto the stimulated sites of the EE during tANS.

The second aim is to develop a set-up that can be mechanically tested.

The third aim is to assess the efficiency of the set-up using a human model. For this purpose, tANS should be performed on healthy female volunteers aiming at eliciting a measurable effect on the respiratory and cardiovascular functions.

2 EXPERIMENTAL PART

2.1 Development of the set-up

2.1.1 Selection of the materials

Commercially available and reusable silicone ear plugs that are used by swimmers (ear plugs, product code: 885037, Slazenger, Shirebrook, United Kingdom) were used as the basis for the development of the ear plugs.

The mechanical and electrochemical characteristics were the criteria for choosing the material for the stimulation (cathodes) of the electrical contact with the skin.

With regard to the electrochemical characteristics, pure platinum was selected as the cathode material because it can activate nerve fibres with predominantly capacitive and faradaic mechanisms.^{10,18,20} However, the properties of a cold-rolled platinum ribbon were considered.¹⁹ Accordingly, a cold-rolled platinum ribbon with a thickness of 0.2 mm and purity of 99.99 w/% was used (Zlatarna Celje d. d., Kersnikova 19, 3000 Celje, Republic of Slovenia).^{13,14}

2.1.2 Crafting of cathodes

The crafting of cathodes comprises several handcraft steps.^{19,20} The first step involves cutting discs with a diameter of 4 mm from the 0.2-mm thick platinum ribbon using a special tool and press. The second step involves forging the discs into 0.8-mm high caps. When completed, the geometric surface of the cathode shown in **Figure 1a** that should be deployed during tANS, also

shown in **Figure 1a**, is 14.58 mm². The third step involves welding lead wires onto the bottom of the spherical cavity of the cathode. As the lead wires of the set-up require high flexibility, a finely stranded, superior-quality, silver-plated, copper conductor wire (type AS155-30-1SJ, Cooner Wire, Chatsworth, CA, USA) was used. The specifications of the wire are as follows:

- Number of conductors – 1#,
- North American – 30 AWG,
- Cable insulation – silicon rubber,
- Cable conductor – silver-plated copper.

For a reliable electrical and mechanical connection between a particular cathode and conduction wire, a capacitive discharge spot welder was used. The spot welder, shown in **Figure 1c**, provided a single high-current pulse. For this purpose, a thyristor powered by a large capacitor discharge was deployed. We used a capacitor of 3 F, which produced a voltage as high as 35 V and could store energy up to 1837.5 W. In the discharging process, all the stored capacitor energy was dumped at once using a thyristor. To ensure appropriate and reproducible welds, however, the thicknesses of the cable and the cap cathode, the type of the welding electrode, and the amount of energy delivered were chosen by the welder on a subjective basis.

With regard to the aforementioned aims, the melting point and electrical resistivity of platinum and pure copper, which were 1769 °C and 10.6 μΩcm (at 25 °C), and 1083.4 °C and 16.78 nΩm (at 20 °C) were the optimum welding conditions.

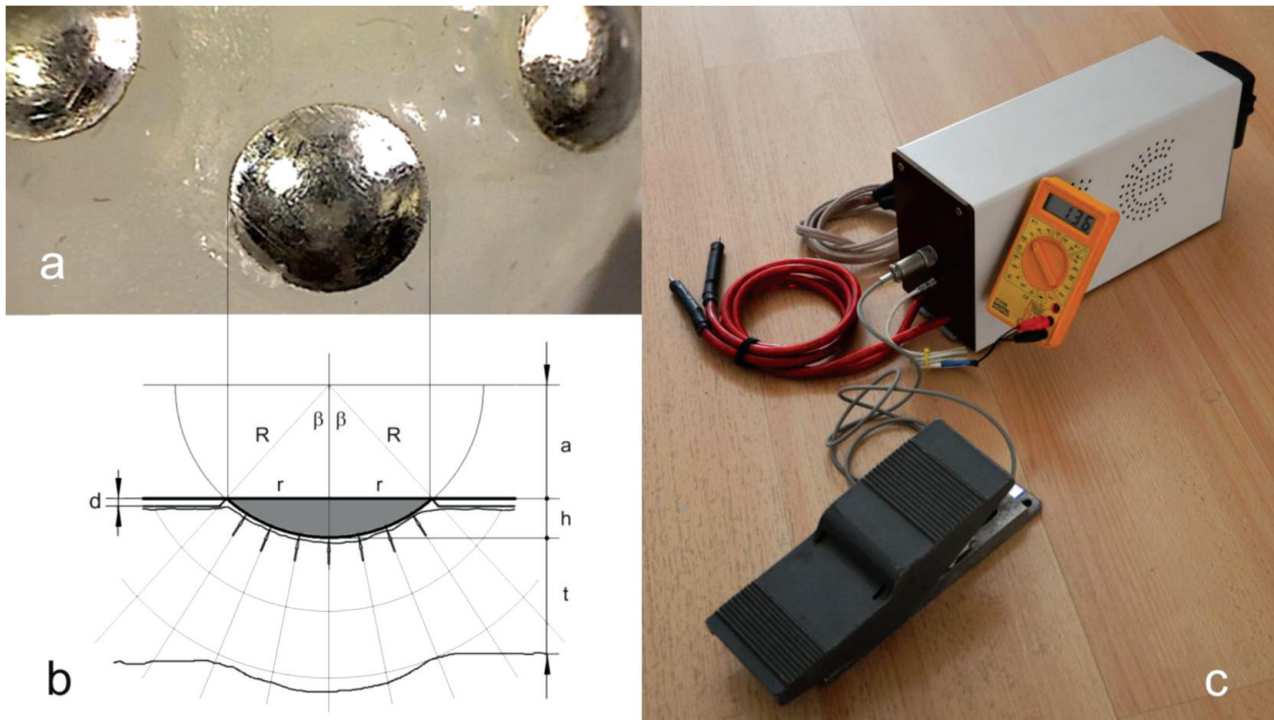


Figure 1: Technology of crafting cathodes: **a)** cup cathode, **b)** cup cathode in contact with skin and an electric field generated by a radially dispersed stimulating current (a – distance, d – silicone insulation thickness, h – cap height, r – cap base radius, R – sphere radius, β – cap angle, t – skin thickness) and **c)** micro-spot-welding device

The monopolar technique was used for welding, and in this process, the electrical current flowed from the positive welding electrode, within the penholder-like handle through the lead wire and spherical cavity, to the negative bulk copper base. To obtain quality welds, wolfram welding electrodes (with a diameter of 3 mm) were customized to obtain a round edge at the tip. During welding, special attention was paid to the pressure applied to the positive electrode. The quality of the weld depended on the internal resistance, achieved by the welder during pressing.

Finally, both silicone plugs were upgraded with four platinum cathodes that were situated at the predefined sites on the tANS model. The cathodes were fixed using a silicone adhesive (ASC, Applied Silicone Corporation, part No.: 40064, MED RTV adhesive, implant grade, Santa Paula, California, USA) that was deposited into the spherical cavity on the back side of the cathode to fill in the cavity and the feedthrough at each predefined site.

The manufactured tANS set-up containing the left and right multi-electrode plugs with four cathodes each is shown in **Figure 2**.

2.2 Mechanical testing

Figure 3 shows a schematic diagram of the assessment of the set-up mechanical performance. **Figure 3a** shows the assessment of axial force F_x versus the bending of the dummy headphone frame and **3b** shows the resulting force F_r acting onto the plug inserted into the EE. To assess the axial force F_x , a digital force gauge (AccuForce Cadet, Ametek, Mansfield & Green Division, Largo, Florida, U.S.A.) was used. Once F_x was measured, the resulting force F_r was calculated using a simple trigonometric function based on the angle of 60° between forces F_x and F_r . This angle was defined by the inclination of the silicone plug where the electrodes were

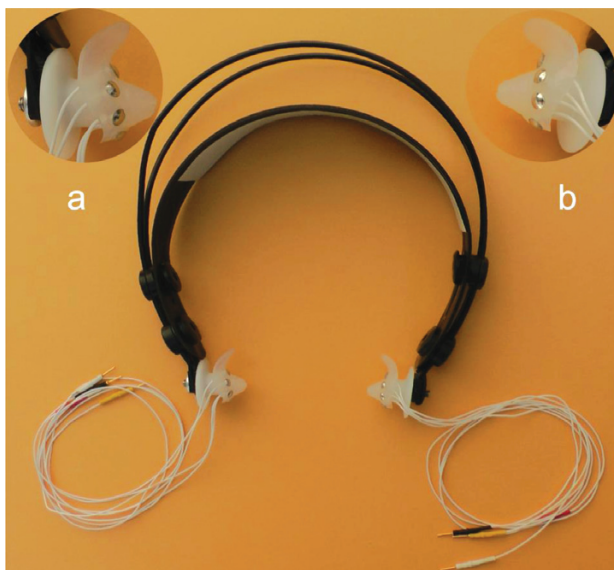


Figure 2: Manufactured tANS set-up; a) left plug; and b) right plug

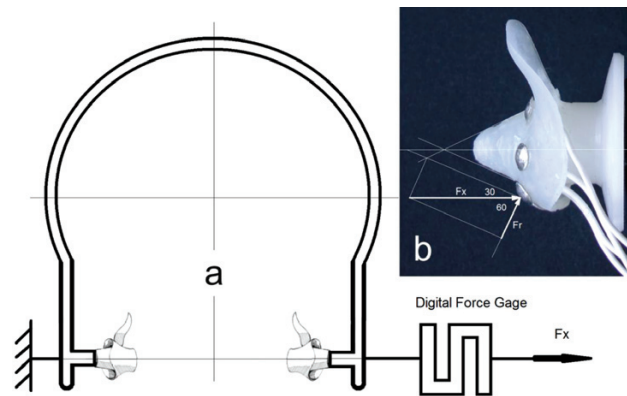


Figure 3: Assessment of the set-up mechanical performance: a) assessment of axial force F_x versus bending of the headphone frame; and b) force F_r resulting from force F_x acting onto the plug at an angle of 60° when inserted into an external ear

situated. Further, the pressure acting onto each cathode, dependent on the bending of the dummy headphone frame when the set-up is mounted onto the head, was calculated.

2.3 Testing the functionality

The primary aim of the testing was to measure the potential impact of multi-electrode tANS of the auricular fibres of the vagus nerve at predefined sites on both EEs on some vital functions of female subjects within an age range of 23–25 years. All subjects were healthy and in ideal physical and psychical conditions. The study was approved by the National Medical Ethics Committee, Ministry of Health, Republic of Slovenia (Tel: +386 01 478 69 13, <http://www.kme-nmec.si/kontakt/>, Unique Identifier No. 0120-297/2018/6).

To protect the subjects against a potential electrical shock, all devices that were in galvanic contact with the subjects were galvanically decoupled from the 220 V power line using a high-quality vintage 500 VA isolation transformer (Mechanikai Laboratórium (ML), Budapest, Hungary).

For the tANS, a certified microprocessor-controlled stimulator (Model SM9079, Shenzhen L-Domas Technology Ltd., Shenzhen, Guangdong, China) (FDA, Medical CE, FCC, ISO13485), was used. The stimuli for the selected tANS were cathodic-first, rectangular current-regulated biphasic stimulating pulse pairs (cathodic and anodic phase). The temporal parameters selected were as follows:

- Frequency – $f = 45.5$ Hz,
- Stimulating phase width – $t_c = 200$ μ s,
- Anodic phase width – $t_a = 200$ μ s,
- On time (pulse train duration) – 3.32 s,
- Time gap between pulse trains – 2.8 s.

The plugs of the tANS set-up with cathodes at the predefined sites were placed into EEs in such a way that each cathode was in contact with the corresponding site at the EE. The stimuli were then delivered to specific

preselected sites at the EE using a custom-developed switching unit situated between the stimulator output and the wires leading to the cathodes.

A common anode (CA), however, was placed at the nape of the neck and connected to another output of the stimulator. As the CA, a reusable and self-adhering neurostimulation electrode (Model: 895240, rectangle of 2" × 3.5", (5 × 9 cm), Axelgaard Manufacturing Co., Ltd., Fallbrook, CA 92028, USA) with a geometric surface of about 4500 mm² was used.

To establish a low-resistance contact between an electrode and sites at the EE, a thin layer of transparent conductive hypo-allergic water-soluble gel (GEL G008, FIAB Spa, Vicchio-Firenze, Italy) was deposited onto the EE.

In our previous study,²⁰ the highest stimulating intensity i_c that produced still acceptable discomfort of the subjects was 50 mA. Accordingly, the i_c of the same intensity (50 mA) was used to evaluate the electrochemical performance of the cathode. The stimulating charge Q_c injected by the test cathode into a site at the EE was obtained by calculating the surface under the cathodic current phase i_c of the stimulating pulse pair:

$$Q_c = i_c \times t_c = 50 \text{ mA} \times 200 \text{ } \mu\text{s} = 10 \text{ } \mu\text{C}, \quad (1)$$

where i_c is the stimulating intensity and t_c is the pulse duration.

The spherical cathode surface area A_c calculated as the average of all eight spheres in the right and left plug is 14.58 mm². The cathodic charge density C_d based on the aforementioned calculations is as follows:

$$C_d = Q_c/A_c = 10 \text{ } \mu\text{C} \div 14.58 \text{ mm}^2 = 0,68 \text{ } \mu\text{C}/\text{mm}^2 \quad (2)$$

The charge transferred by a particular cathode was the same but opposite to the charge transferred by the CA, while the charge densities differed vastly. Accordingly, the charge density A_d transferred by the CA is as follows:

$$A_d = Q_c/A_a = 10 \text{ } \mu\text{C} \div 4,500 \text{ mm}^2 = 2,22 \text{ nC}/\text{mm}^2 \quad (3)$$

To characterize the interface between the four cathodes located at the left and right EEs, ensemble variables, such as capacitance C_e and parallel resistance R_e , were measured using an LCR meter (AT2816A Precision Digital LCR Meter, Changzhou Applent Instruments, Ltd., Jiangsu, China). The measuring conditions were as follows:

- Source resistance – 30 Ω,
- Testing excitation voltage – 1 V,
- Testing frequency – 1.2 kHz.

The testing frequency of 1.2 kHz was extracted from the power spectrum density of the stimulation pulse (not shown in this paper).

Electroimpedance measurements (single cathode vs. large CA) were attempted while the electrodes were worn by the subjects. To protect the subjects against a potential electrical shock, the LCR meter was galvanically

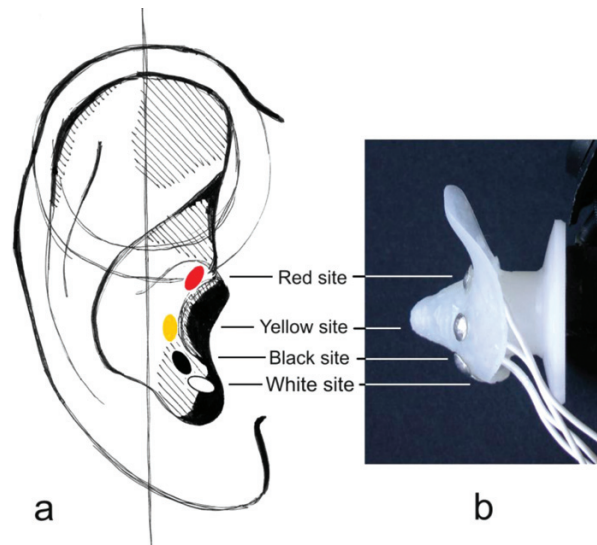


Figure 4: Testing the functionality: a) right plug; b) predefined stimulating sites on the right EE

cally decoupled from the 220 V power line using the aforementioned vintage isolation transformer.

Figure 4 shows a schematic diagram of testing the set-up functionality. **Figure 4** also shows the sites on the right EE that were predefined for the tANS. They were indicated in the following order: pole position, red (R); below pole position, yellow (Y); above bottom position, black (B); and bottom position, white (W).

For the measuring set-up, various custom-designed and commercially available devices were used so that the following physiological quantities could be measured:

- tANS intensity – i_c ,
- Phonothrographic signal – PTG,
- Phonocardiographic signal – PCG,
- Heart rate – HR,
- Airflow – AF,
- Toe photoplethysmographic signal – PPG,
- Blood pressure – BP,
- Korotkoff sounds – KS.

2.3.1 Measurement of the airflow in nasal ventilation

An airflow (AF) measuring system was used to assess the variations in the pressure difference elicited by the bi-directional total nasal AF,²¹ changes in the rhythm, and the changes in the character of inhalation and exhalation produced by the selective tANS. The system comprised a full face mask (iVolve Full Face Mask, BMC Medical Co., Ltd., Shijingshan, Beijing, China) and a mass AF meter (FS6122-100F100-5P40-TH1, NONCON, Hubei, China) designed for personal ventilators for continuous positive airway pressure. The specifications of this system were as follows:

- Airflow range – -100 ~+ 100 SLPM,
- Accuracy – ± (2.0 + 0.5 FS) %,
- Output mode – Linear analogue VDC,
- Output range – 0.5 ~ 4.5 VDC,

- Response time – 1.8 ms.

In the resulting bi-direction AF curve, the horizontal line denotes zero airflow, positive AF values correspond to periods of inhalation, and negative AF values correspond to periods of exhalation.

2.3.2 Capturing heart rate and the toe plethysmographic signal

To study the impact of the tANS on a subject's heart metrics, photo-plethysmography was used. Accordingly, to capture the toe photo-plethysmographic waveforms (PPG) during the selective tANS, a pulse oximeter (Nellcor N-595, SpO₂ accuracy of $\pm 2\%$ (90–100 %), $\pm 3\%$ (70–89 %), pulse rate accuracy of ± 1 bpm (30–90 bpm), 2 bpm (60–149 bpm), 3 bpm (150–245 bpm), Tyco Healthcare Group LP, Nellcor Puritan Bennett Division, Pleasanton, CA, U.S.A.), instrumented with a custom-crafted PPG toe clip, was used. An IR LED pair and photodiode taken from a commercially available SpO₂ sensor (Model Number: CSL032H, Nellcor DOC-10, Oximax Animal Ear Clip SpO₂ Sensor for Nellcor N-595, Certificates CE and ISO13485, Shenzhen YKD Technology Co., Ltd., Brand Name: YONGKANGDA, Guangdong, China) were attached to two halves of a tube, made of carbon fibre so that they face the lower and upper side of the toe, respectively. The toe clip was used to capture both the heart rate (HR) and PPG from the cardiac cycle, referring to the contraction and relaxation of the ventricles while attached onto the left toe. To reduce the noise from the motion, and obtain an optimum signal representing a distinguished dicrotic notch, a no low-pass filter was applied. The optimum filter for the PPG processing was already applied to the pulse oximeter. The average of the HR was calculated from fifteen peaks of KS within the BP intervals that were recorded before, during and after tANS.

2.3.3 Capture of Korotkoff sounds and phonothreographic signal

The system used for capturing the phonothreogram (PTG) and Korotkoff sounds (KSs) included a precision active contact acoustic transducer (CM-01B, Shenzhen Aimin Intelligent Technology Co., Ltd., Shenzhen, China) and a signal amplifier module (CM-01, Shenzhen Aimin Intelligent Technology Co., Ltd., Shenzhen, China). The specifications of the system were as follows:

- Sensitivity – 40 mV/mm,
- Lower limit frequency (–3dB) – 8 Hz,
- Upper frequency (+3dB) – 2.2 kHz,
- Output voltage range – 0–1.215 mV.

The two aforementioned combinations were attached onto the custom-designed frame pieces; one is designed as a necklace and the other is designed as an upper arm cuff. The transducer was calibrated at quiet normal room sound conditions, with an estimated peak-to-peak sound of approximately 25 dB.

The KSs were captured using the transducer placed over the brachial artery simultaneously with the mea-

surement of BP using the cuff^{22–25} while the PTG representing a bruit coming out from the thyroid vasculature was captured using the transducer placed above the thyroid isthmus.

2.3.4 Measurement of blood pressure

The oscillometric method was used to measure BP, and with this method, the cuff was wrapped around the left upper arm. The brachial artery, which was constricted by an inflated cuff, was used as the primary vessel. The BP value needed as the calibration reference in the BP measurement was measured manually with a commercially available appliance (Oberarm-Blutdruckmessgerät MD 12450, salvatec, Essen, Germany) and a proprietary cuff, which were attached to the area around the left upper arm. The specifications of the device were as follows:

- BP range – 30–250 mmHg,
- Pulse range – 40–180 beats/minute,
- BP accuracy – ± 3 mmHg,
- Pulse accuracy – $\pm 5\%$ of value displayed.

The pressure within the BP cuff was measured using a pressure transducer (type 4-327-C, range: 0–400 mmHg, Beckman Instruments Inc., Fullerton, CA, U.S.A.), which was situated between the aforementioned cuff and the appliance.

To calibrate the pressure transducer, a digital non-invasive sphygmomanometer calibrator (SLK-BXY-250, Shelok, Shaanxi, China), situated between the cuff manual pump and pressure transducer, was used. The specifications of the device were as follows:

- Pressure range – 0–40 kPa,
- Accuracy – 0.16 %.

2.3.5 Capturing the phonocardiographic signal

The phonocardiographic signal (PCG) associated with heart sounds²³ was captured in real-time using a custom-modified stethoscope comprising an auscultation headset²⁴ with a diameter of 41 mm. The headset consisted of a diaphragm, which was the sensing part of the stethoscope, and a head, onto which an electret condenser microphone (CMA-4544PF-W, CUIINC, Tualatin, Oregon, USA) was fitted. To add an "ear" to the headset, an assembled low-noise microphone amplifier module (GY-MAX4466, MINGYUANDINGYE, China) instrumented with a Maxim MAX4466 operational amplifier, specifically designed for this delicate task, was used. The gain could be adjusted between 25 \times and 125 \times using a small trimmer potentiometer. The device specifications were as follows:

- Frequency range – 20–20,000 Hz,
- Analogue signal output – 0.2–1 V,
- Output signal bias – VCC/2 DC.

This module actually came with a wide bandwidth omnidirectional electret condenser. Its specifications include the following:

- Sensitivity – -44 ± 2 dB, $f = 1$ kHz, 1 Pa 0 dB = 1 V/Pa,
- Operating frequency – 20~20,000 Hz,
- Signal-to-noise ratio – 60 dBA, $f = 1$ kHz, 1 Pa A-weighted.

To capture the two main heart sounds for the PCG analysis, namely S1 and S2,²⁴ a stethoscope is placed at the fifth auscultation area, known as the mitral area or apex area (M) above the cardiac apex.²⁴

2.3.6 Assessment of respiratory sinus arrhythmia

The respiratory sinus arrhythmia (RSA) was assessed during bi-nasal and bi-directional breathing before, during, and after the tANS at a relaxed non-forced rate. Precisely, the sinus arrhythmia ratio (E/I) was calculated by dividing the longest with the shortest interval, extracted from the fifteen peaks of KS within the BP intervals recorded before, during, and after the tANS.

During the 20-min test period, tANS was applied using each of the four cathodes of the left and right plugs. Each 20-min test period started with a 5-min sham segment when stimulating pulses were not delivered (sham I), proceeded with a 10-min tANS segment, and ended with another 5-min sham segment (sham II). During the testing, the stimulating intensity i_c was pre-set by the subject using the dial on the electrical stimulator until minimum discomfort at the particular site below the deployed cathode was detected.²⁰

2.3.7 Ending the experiment

The first step in ending the experiment was minimizing the i_c and turning the stimulator off. Then, the subject remained lying supine on the chair for additional 10 min so that the sensory and stimulating components could be removed. The first and the most delicate component removed was the tANS set-up. At the same time, the CA placed at the nape of the neck was removed. The second component removed was the full face mask with the mass AF meter. The third component removed was the BP cuff wrapped around the subject’s left arm. The fourth component removed was the SpO2 sensor placed on the left toe. The components removed last were the PCG stethoscope and PTG active contact acoustic transducer.

Finally, the skin at the EE sites and the skin at the back cervical neck was degreased with 70 % isopropyl alcohol and let to dry.

2.3.8 Signal pre-processing and acquisition

All the analogue signals coming from the sensors were prepared for the identification of important signal features, whilst avoiding false identification. In this procedure, the type and order of the applied filter were selected. Each of the eight signals coming from the conditioning circuits was digitized at 50 kHz with a 24-bit resolution using a high-performance I/O data-acquisition system (DEWE-43, DEWESOFT d. o. o., Republic of Slovenia) and the acquisition software (DEWESoft

7.0.2) Finally, the data were stored on a portable computer (Lenovo W541, Lenovo, Beijing, China) for further signal processing.

In an offline analysis, the average of the quantities that were extracted from the waveforms within sham I, during the tANS and within sham II always contained the proprietary BP waveform.

Finally, **Figure 7** was constructed to represent groups of columns/quantities describing: experimental conditions, respiratory function, cardiovascular function, and the effect.

3 RESULTS

The ensemble variables, namely capacitance C_e and parallel resistance R_e , representing an interface between each of the four cathodes when located at the left and right EE and the CA, are shown in **Table 1**.

Table 1: Average of the interfacial ensemble variables

	C_e (nF)	R_e (k Ω)
Average	3.9	37.86

The results of the mechanical testing depicted in **Figure 5** show that the pressure on each stimulating electrode is almost linearly dependent on the bending of the headphone frame.

The results of testing the functionality are depicted in **Figure 6**.

These results are represented through waveforms of the quantities recorded for one of the participants during the selective tANS of the site at the bottom (see **Figure 4**) of the right EE marked with white colour. The waveforms of the quantities are indicated in the following order (from top to bottom): i_c , PTG, PCG, HR, AF, PPG, BP and KS.

Figure 7 shows an example of the most apparent effects of the selective tANS of the RW site on the two vital physiological functions. Precisely, **Figure 7** contains

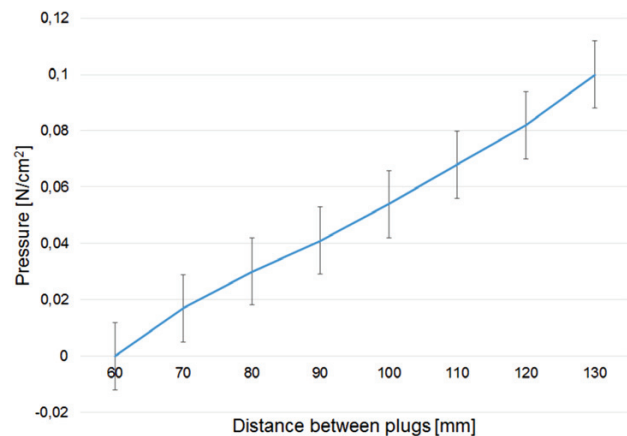


Figure 5: Pressure acting on the stimulating electrode according to the bending headphone frame when the set-up is mounted onto the head

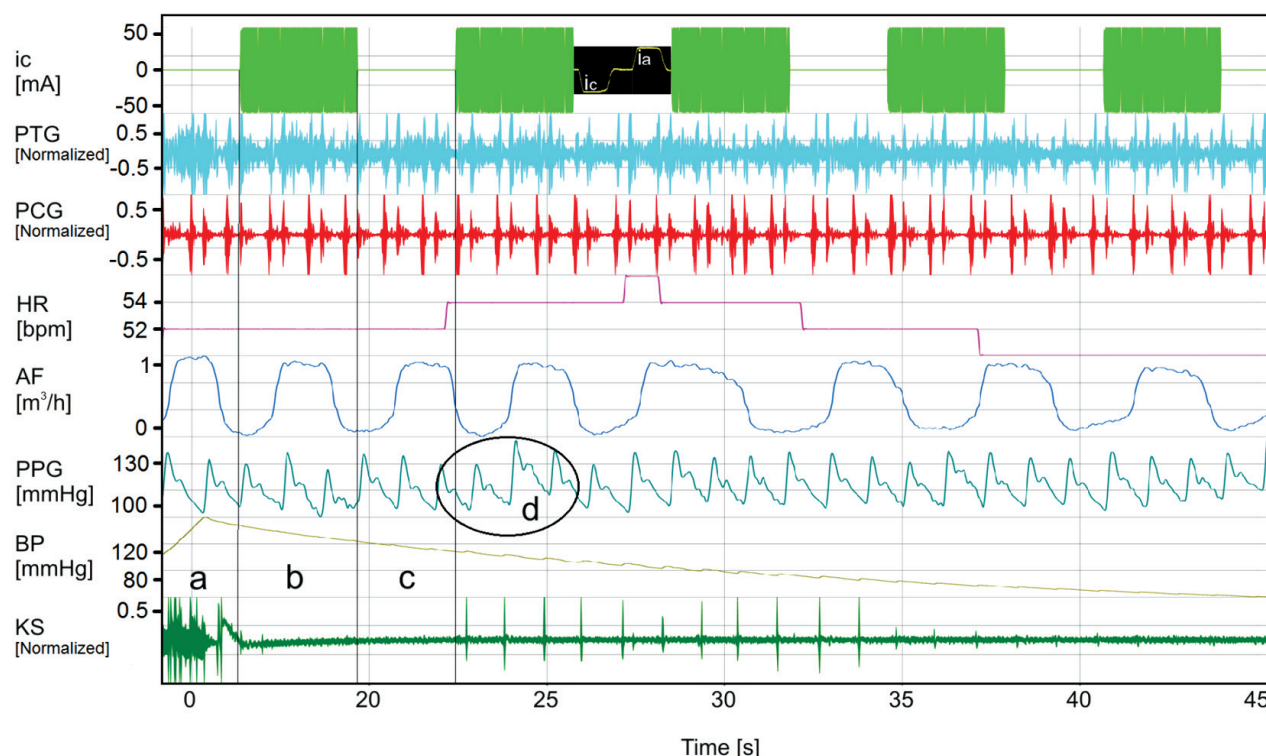


Figure 6: Quantities recorded during selective tANS of RW (from top to bottom): i_c (train of pulses and detailed shape of pulses); PTG; PCG; HR; AF; PPG; BP and KS; a) sham I; b) tANS; c) sham II; d) low amplitude masking waves

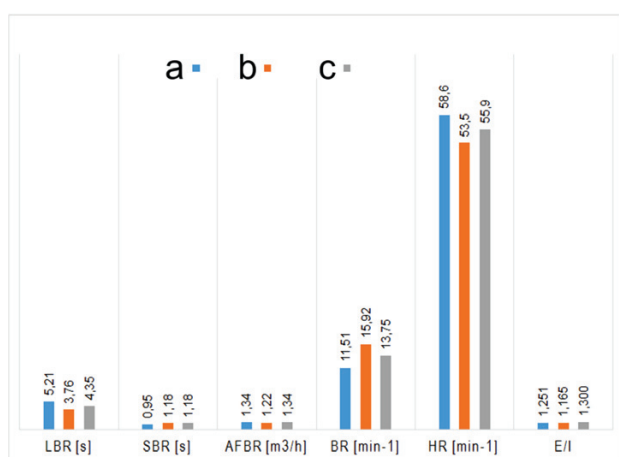


Figure 7: Average of the most indicative effects of selective tANS of the right white site: a) sham I (blue); b) tANS at $i_c = 57.3$ mA (red); c) sham II (grey)

averaged values of the effects elicited onto the respiratory and cardiovascular functions during sham I, tANS of the RW site, and sham II.

4 DISCUSSION

The findings of the study are consistent with the published results of other investigators^{25–27}. However, compared to other systems, the developed four-electrode set-up is more favourable because of its ability to provide tANS using any combination of the four stimulating

electrodes at the plug without the need to change the location of the physical electrode.

The spatial selectivity, however, is strongly dependent on the position of the electrodes above the nerve endings located within a particular site at the EE as well as on stimulating parameters.

The set-up was developed in such a way that it enables several possibilities for determining better stimulating sites, using different electrode arrangements, and using a variety of stimulating parameters. There is a vast stimulating parameter space, which is closely related to the temporal conditions and stimulating conditions.

A major weakness of the developed set-up is the fact that the tANS efficiency is significantly dependent on the pressure applied to the electrodes and generated by the headphone frame.

The factor that contributed the most toward understanding the problem with tANS is that tANS was delivered monopolarly to four particular sites on the EE that are innervated predominantly by the fibres of the auricular nerve.²⁷ Namely, no studies have addressed the effects of the tANS of the EE using a single-part set-up containing multiple platinum-stimulating electrodes.

The results obtained with mechanical testing showed that the pressure exerted by a particular electrode onto the EE during tANS, while simulating the head fitment, was within a range of 0–9.8 N/cm² (see **Figure 5**).

This pressure was deemed appropriate for the tANS. During the short-term tANS, the set-up was rated good by all subjects, and no side effects were noticed.

Table 2: Potential effects of the tANS on the quantities related to the two vital physiological functions

Physiological function	Quantity	Description of tANS effect on the quantity
Respiratory function	LBR	The length of binasal respirations shortened by 27 % during the tANS and changed to 16.5 % below the initial value during sham II.
	SBR	The slope of binasal respirations was enlarged by 24.21 % during the tANS and remained at this value during sham II.
	AFBR	The airflow of binasal respirations diminished by 8.95 % during the tANS and returned to the initial value during sham II.
	BR	The breathing rate was enlarged by 38.31 % during the tANS and returned to 19.46 % above the initial value during sham II.
Cardiovascular function	HR	The heart rate diminished by 8.7 % during the tANS and returned to 4.6 % below the initial value during placebo II.
	E/I	The respiratory sinus arrhythmia ratio diminished by 6.87 % during the tANS and increased to 3.91 % above an initial value during sham II.
	PPG	PPG exhibited two features, namely peak systolic perfusion and the start of the next systole. However, unlike the normal PPG waveform observed within the time periods without tANS, an underdamped like PPG waveform was observed within the time periods with tANS. Namely, a slightly narrow peak systolic PPG, deep dicrotic notch and non-physiological oscillations with a frequency of approximately 300 min ⁻¹ during the diastolic phase were observed. ²⁸⁻³⁰ This effect may be attributed to tachydysrhythmia. ³⁰ This assumption was confirmed with the PPG trace in Figure 6 , which showed a slightly narrow peak systolic PPG, deep dicrotic notch and non-physiological oscillations during the tANS solely.

In **Table 2**, preliminary results obtained when testing functionality are presented. To interpret these results, short descriptions of the effects of the tANS on the quantities related to the two assessed vital physiological functions during the 10-min tANS and sham II are provided.

It was shown that the results obtained with mechanical testing correlated to those obtained with functionality testing.

However, due to a low number of subjects tested and trials performed, the results representing the changes in physiological variables shown in **Table 2** should be considered as the basis for further research activities and not as the basis for credible conclusions. Further research, necessary for addressing the issues highlighted in these preliminary results, could proceed in the following directions:

- to introduce computational models incorporating theoretical and experimental insights,
- to accomplish a more detailed analysis of tANS effects,
- to develop a set-up with even more stimulating cathodes, thus providing the tANS at more sites on the EE,
- to systematically study the mechanism of actions and optimal tANS modalities,
- to improve the stimulating electrode/skin contact.

The next step in our study could comprise the following tasks:

- to assess other vital physiological functions,
- to evaluate the interaction between different physiological functions upon tANS,
- to perform more experiments to show group statistics.

Our aim was to develop a set-up with appropriate mechanical features so that it is capable of generating an

optimum pressure for the stimulating sites at the EE during tANS.

During tANS, an adequate cathode/skin contact was made, ensuring that a high i_c density, potentially eliciting skin irritation, was avoided.³¹ The maximum i_c of 50 mA applied to a preselected site is rather high. However, to obtain a tANS effect on a particular internal organ, one needs to activate the nerve endings located at a distance from the skin surface. Precisely, the dV/dt ratio needs to be high enough at particular nerve endings so that the resulting function is capable to depolarize the nerve endings. Subthreshold currents, however, do not depolarize nerve endings. Besides, a relatively large amount of voltage is needed to overcome electroporation, so the i_c must elicit a voltage drop high enough to overcome both of the aforementioned voltages.

Most importantly, the selective tANS of the predefined sites on the EE elicited a measurable effect on both the cardiovascular and respiratory functions of female subjects.

We believe that the present study contributes to the further development of multi-electrode set-ups that could help transfer the tANS technique into clinical practice as a relevant therapy.

5 CONCLUSIONS

The presented work has implications for the design of a multi-electrode set-up, and the prediction of a long-term tANS efficacy. Furthermore, an increased number of channels may extend the application of tANS, potentially enhancing its performance and autonomic function and modifying some other physiological functions.^{26,27}

Acknowledgement

The authors acknowledge the financial support from the Slovenian Research Agency (Research core funding No. P3-0171).

6 REFERENCES

- ¹ A. Kuhn, Modeling transcutaneous electrical stimulation, Diss. ETH No. 17948, ETH Zurich, Zurich 2008, 211
- ² J. Ellrich, Transcutaneous vagus nerve stimulation, *Eur. Neurol. Rev.*, 6 (2011) 4, 254–6, doi:10.17925/ENR.2011.06.04.254
- ³ D. R. McNeal, Analysis of a model for excitation of myelinated nerve, *IEEE Trans. Biomed. Eng.*, 23 (1976) 4, 329–337, doi:10.1109/tbme.1976.324593
- ⁴ F. Rattay, Analysis of models for external stimulation of axons, *IEEE Trans. Biomed. Eng.*, 33 (1986) 10, 974–977, doi:10.1109/TBME.1986.325670
- ⁵ M. F. Butt, A. Albusoda, A. D. Farmer, Q. Aziz, The anatomical basis for transcutaneous auricular vagus nerve stimulation, *Journal of Anatomy*, 236 (2020) 4, 588–611, doi:10.1111/joa.13122
- ⁶ B. W. Badran, O. J. Mithoefer, C. E. Summer, N. T. LaBate, C. E. Glusman, A. W. Badran, W. H. DeVries, P. M. Summers, C. W. Austelle, L. M. McTeague, J. J. Borckardt, M. S. George, Short trains of transcutaneous auricular vagus nerve stimulation (taVNS) have parameter-specific effects on heart rate, *Brain Stimul.*, 11 (2018) 4, 699–708, doi:10.1016/j.brs.2018.04.004
- ⁷ E. Frangos, J. Ellrich, B. R. Komisaruk, Non-invasive access to the vagus nerve central projections via electrical stimulation of the external ear: fMRI evidence in humans, *Brain Stimul.*, 8 (2015) 3, 624–36, doi:10.1016/j.brs.2014.11.018
- ⁸ L. Grazzi, S. Usai, G. Bussone, Gammacore device for treatment of migraine attack: preliminary report, *J. Headache Pain*, 15 (2014) 1, G12–G12, doi:10.1186/1129-2377-15-S1-G12
- ⁹ F. Huang, J. Dong, J. Kong, H. Wang, H. Meng, R. B. Spaeth, S. Camhi, X. Liao, X. Li, X. Zhai, S. Li, B. Zhu, P. Rong, Effect of transcutaneous auricular vagus nerve stimulation on impaired glucose tolerance: a pilot randomized study, *BMC Complement. Altern. Med.*, 14 (2014) 203, doi:10.1186/1472-6882-14-203, Erratum in, *BMC Complement. Altern. Med.*, 16 (2016) 1, 218, doi:10.1186/s12906-016-1190-1
- ¹⁰ E. M. Hudak, J. T. Mortimer, H. B. Martin, Platinum for neural stimulation: voltammetry considerations, *J. Neural Eng.*, 7 (2010) 2, 26005, doi:10.1088/1741-2560/7/2/026005
- ¹¹ P. Battaini, Electrolytic Etching for Microstructure Detection in Platinum Alloys, *Platinum Metals Review*, 55 (2011) 1, 71–72, doi:10.1595/147106711X540706
- ¹² P. Battaini, Microstructure Analysis of Selected Platinum Alloys, *Platinum Metals Review*, 55 (2011) 2, 74–83, doi:10.1595/147106711X554008
- ¹³ J. C. Wright, Jewellery-Related Properties of Platinum. Low thermal diffusivity permits use of laser welding for jewellery manufacture, *Platinum Metals Review*, 46 (2002) 2, 66–72
- ¹⁴ K. Toyoda, T. Miyamoto, T. Tanihira, H. Sato (inventors), Pilot Pen Co Ltd, High Purity Platinum and its Production, Japanese Patent 7/150, 271, 1995
- ¹⁵ L. F. Jeffus, *Welding: Principles and Applications*, 6th ed., Delmar Cengage Learning, New York 2007
- ¹⁶ G. Shannon, Advances in Resistance Welding Technology Offer Improved Weld Quality and Reliability for Battery Manufacturers, *Battery Power Products & Technology*, 11 (2007) 4
- ¹⁷ G. F. Schrader, A. K. Elshennawy, *Manufacturing Processes & Materials*, Society of Manufacturing Engineers, Dearborn 2000
- ¹⁸ L. S. Robblee, T. L. Rose, The electrochemistry of electrical stimulation, Proc. of the 12th Annual International Conference of the IEEE Engineering in Medicine & Biology Society, Philadelphia 1990, 1479–1480
- ¹⁹ Y. N. Loginov, A. V. Yermakov, L. G. Grohovskaya, G. I. Studenok, Annealing Characteristics and Strain Resistance of 99.93 wt.% Platinum. Implications for the manufacture of platinum artefacts, *Platinum Metals Review*, 51 (2007) 4, 178–184, doi:10.1595/147106707x237708
- ²⁰ J. Rozman, L. Stojanovic, S. Ribarič, Short-term effects of selective transcutaneous auricular-nerve stimulation measured in a subject with angina pectoris, *Materials and Technology*, 55 (2021) 3, 387–399, doi:10.17222/mit.2021.011
- ²¹ A. A. T. Borojeni, G. J. M. Garcia, M. Gh. Moghaddam, D. O. Frank-Ito, J. S. Kimbell, P. W. Laud, L. J. Koenig, J. S. Rhee, Normative ranges of nasal airflow variables in healthy adults, *Int. J. Comput. Assist. Radiol. Surg.*, 15 (2020) 1, 87–98, doi:10.1007/s11548-019-02023-y
- ²² D. A. Sykes, K. McCarty, E. Mulkerrin, D. J. Fisher, J. P. Woodcock, Correlation between Korotkoff's sounds and ultrasonics of the brachial artery in healthy and normotensive subjects, *Clin. Phys. Physiol. Meas.*, 12 (1991) 4, 327–31, doi:10.1088/0143-0815/12/4/002
- ²³ R. J. Oweis, H. Hamad, M. Shammout, Heart Sounds Segmentation Utilizing Teager Energy Operator, *Journal of Medical Imaging and Health Informatics*, 4 (2014) 4, 488–499(12), doi.org/10.1166/jmhi.2014.1292
- ²⁴ C. Ahlström, Processing of the Phonocardiographic Signal - Methods for the Intelligent Stethoscope, Linköping Studies in Science and Technology, Thesis No. 1253, Linköping University, Institute of Technology, Linköping 2006
- ²⁵ T. R. Henry, Therapeutic mechanisms of vagus nerve stimulation, *Neurology*, 59 (2002) 6, Suppl. 4, S3–S14, doi:10.1212/wnl.59.6_suppl_4.s3
- ²⁶ J. A. Clancy, D. A. Mary, K. K. Witte, J. P. Greenwood, S. A. Deuchars, J. Deuchars, Non-invasive vagus nerve stimulation in healthy humans reduces sympathetic nerve activity, *Brain Stimulation*, 7 (2014) 6, 871–877, doi:10.1016/j.brs.2014.07.031
- ²⁷ E. T. Peuker, T. J. Filler, The nerve supply of the human auricle, *Clin. Anat.*, 15 (2002) 1, 35–7, doi:10.1002/ca.1089
- ²⁸ E. Burns, R. Buttner, Ventricular Fibrillation, <https://litfl.com/ventricular-fibrillation/>
- ²⁹ Mayo Clinic, Atrial flutter, <https://www.mayoclinic.org/diseases-conditions/atrial-flutter/symptoms-causes/syc-20352586>
- ³⁰ S. Rezaie, Damping and Arterial Lines, <https://rebelem.com/damping-and-arterial-lines/>
- ³¹ B. W. Badran, A. B. Yu, D. Adair, G. Mappin, W. H. DeVries, D. D. Jenkins, M. S. George, M. Bikson, Laboratory Administration of Transcutaneous Auricular Vagus Nerve Stimulation (taVNS): Technique, Targeting, and Considerations, *J. Vis. Exp.*, 143 (2019), e58984, doi:10.3791/58984